CHEMISTRY
AN ASIAN JOURNAL

DOI: 10.1002/asia.200600411

Coupling between Substituents as a Function of Cage Structure: Synthesis and Valence Ionized States of Bridgehead Disubstituted Parent and Hexafluorinated Bicyclo[1.1.1]pentane Derivatives $C_5X_6Y_2$

Masahiro Ehara,*[a] Shuhei Fukawa,[a] Hiroshi Nakatsuji,[a] Donald E. David,[b] Evgueni Z. Pinkhassik,[b] Michael D. Levin,[b] Marcin Apostol,[b] and Josef Michl*[b]

Dedicated to Professor Neil Bartlett on the occasion of his 75th birthday

Abstract: He(I) photoelectron spectroscopy was used to examine the valence-shell electronic structure of three new and seven previously known bicyclo[1.1.1]pentane derivatives, 1,3-Y_2-C_5X_6 (for X = H, Y = H, Cl, Br, I, CN; for X = F, Y = H, Br, I, CN). A larger series (X = H or F, Y = H, F, Cl, Br, I, At, CN) has been studied computationally with the SAC-CI (symmetry-adapted cluster configuration interaction) method. The outer-valence ionization spectra calculated by the SAC-CI method, including spin–orbit interaction, reproduced the experimental photoelectron spectra well, and quantitative assignments are given. When the extent of effective through-cage interaction between the bridgehead halogen lone-pair orbitals was defined in the usual way by orbital-energy splitting, it was found to be larger than that mediated by other cages such as cubane, and was further enhanced by hexafluorination. The origin of the orbital-energy splitting is analyzed in terms of cage structure, and it is pointed out that its relation to the degree of interaction between the bridgehead substituents is not as simple as is often assumed.

Keywords: ab initio calculations · electronic structure · photoelectron spectroscopy · through-bond interactions · through-space interactions

Introduction

The indirect interaction of two molecular constituents Y′ and Y″ mediated by an "inert" coupler Z (through-bond coupling, superexchange)[1–9] has long been studied in the realm of electron and energy transfer, and has generated renewed interest in the context of molecular electronics, in which both highly conducting and strongly insulating moieties Z are needed. It is also relevant for the propagation of substituent effects, NMR and EPR coupling constants, heavy-atom effects on spin–orbit coupling, and other phenomena affected by sigma-electron delocalization.

In spite of well-documented shortcomings, it is usually advantageous for qualitative insight and conceptual understanding to interpret photoelectron spectra (PES) of organic molecules in terms of Hartree–Fock orbital energies and the Koopmans' theorem, ignoring spin–orbit coupling even in the presence of atoms of relatively high atomic number. Presently, we have combined this intuitive approach with the use of a more quantitative analysis based on the calculation of state energies by using the correlated SAC/SAC-CI (symmetry-adapted cluster configuration interaction) method[10–13] with inclusion of spin–orbit coupling at equilibrium structures optimized by the MP2 method. This permitted unambiguous assignment of the valence-shell PES, which used to be much more tentative,[14–17] and thus a reliable evaluation of the Y′–Y″ interactions mediated by the coupler. The SAC-CI SD-*R* method, in which the linked ion-

[a] Assoc. Prof. M. Ehara, S. Fukawa, Prof. H. Nakatsuji
Department of Synthetic Chemistry and Biological Chemistry
Graduate School of Engineering, Kyoto University
Katsura, Nishikyo-ku, Kyoto 615-8510 (Japan)
Fax: (+81) 75-383-2759
E-mail: ehara@sbchem.kyoto-u.ac.jp

[b] Dr. D. E. David, Dr. E. Z. Pinkhassik, Dr. M. D. Levin, Dr. M. Apostol, Prof. J. Michl
Department of Chemistry and Biochemistry
University of Colorado
Boulder, CO 80309-0215 (USA)
Fax: (+1) 303-492-0799
E-mail: michl@eefus.colorado.edu

Supporting information for this article is available on the WWW under http://www.chemasianj.org or from the author.

ization operators consist of single- and double-excitation operators, is known to reproduce the primary peaks in the outer-valence region of small molecules quite accurately.[18–24]

It has become standard to use the splitting $\Delta E = E(\psi^+) - E(\psi^-)$ of the ionization energies E of the in-phase (ψ^+) and out-of-phase (ψ^-) combination of orbitals $\psi_{Y'}$ and $\psi_{Y''}$ localized on the two equivalent substituents Y′ and Y″, respectively, as a quantitative measure of the effectiveness of an intervening coupler cage in providing an indirect coupling mechanism when direct through-space coupling of Y′ with Y″ is negligible due to their large distance. This is usually justified by pointing to the two-dimensional nature of the problem when Y'^+–cage–Y″ and Y′–cage–Y''^+ are the only two electron configurations that need to be considered. In the ordinary molecular-orbital approximation, the effective resonance integral β_{YY}^{cage} that describes the effect of coupling through the cage is then equal to $\Delta E/2$. We offer a straightforward rationalization of the widely varying values of β_{YY}^{cage} for constant Y as a function of the structure of the cage. However, we also conclude that β_{YY}^{cage} defined in this way does not have the simple meaning usually attributed to it, as the only instance for which electron configurations of the type Y′–$cage^+$–Y″ can be safely ignored is if there is no through-bond coupling. Cases of interest are therefore of more than two dimensions, and the usual analysis is of questionable value.

Because of their rigidity, bicyclic and polycyclic hydrocarbon cages such as bicyclo[2.2.2]octane and cubane have been of particular interest. The bicyclo[1.1.1]pentane (**1**) skeleton[25] (Figure 1) seems to be particularly effective as a

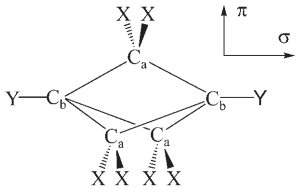

	X	Y
1:	H	H
1,3-Y_2-**1**:	H	Y
2:	F	H
1,3-Y_2-**2**:	F	Y

Figure 1. Molecular structure of $C_5X_6Y_2$ (X = H, F; Y = H, F, Cl, Br, I, At, CN) and definitions of atoms, directions, and the system of compound naming.

through-bond coupler. It is of interest both as a rod or bridge unit for molecular construction kits[26] and because of its unusual electronic structure. There is considerable transannular (through-space) interaction between the bridgehead carbon atoms, which are not linked by a bond although they are less than 2 Å apart; through-bond coupling involving the highly strained C–C bonds between bridgehead and bridge carbon atoms is strong as well. Spectroscopic and computational evidence for bridgehead–bridgehead interactions in **1** has been reviewed.[25] NMR[27] and EPR[28] coupling constants demonstrated interactions between σ-symmetry bridgehead orbitals, whereas in the hands of Gleiter et al.[14] the PES of a few of these compounds provided evidence for similar interactions between bridgehead orbitals of π symmetry. We report herein an update and considerable extension of the brief note of Gleiter et al.[14] on the PES of bridgehead-substituted bicyclo[1.1.1]pentanes, and also examine their hexafluoro derivatives.

The present combined He(I) photoelectron spectroscopy and computational study thus provides a more thorough characterization of the transmission of electronic interactions through the bicyclo[1.1.1]pentane cage. It takes advantage of the threefold symmetry of the structures Y–C_5H_6–Y (1,3-Y_2-**1**; Y = H, F, Cl, Br, I, CN) and their hexafluoro analogues Y–C_5F_6–Y (1,3-Y_2-**2**) to examine the clearly apparent effects of spin–orbit coupling in the ionized state, from Y = F to Y = At. The examination of the effects of perfluorination has long been known[29] as a useful tool for the interpretation of PES. In bicyclo[1.1.1]pentanes, it also increases the interbridgehead distance[30] and is therefore likely to have a structural effect on transannular interactions.

An intuitive approach is used to provide a simple but general analysis of the origin of the different ability of various cages to mediate the coupling of bridgehead substituents.

Results

Synthesis

Small amounts of several new hexafluorinated bicyclo[1.1.1]pentanes were prepared specifically for this study. Hexafluorobicyclo[1.1.1]pentane (**2**) was synthesized by the reduction of 1,3-Br_2-**2**[30] with tris(trimethylsilyl)silane and was chlorinated to yield 1,3-dichlorohexafluorobicyclopentane (1,3-Cl_2-**2**). The photochemical chlorination was unusually slow and had to be run for two weeks to yield a sufficient amount of product. The difficulty of the hydrogen abstraction process is undoubtedly due to a combination of the high s character of the exocyclic bridgehead orbitals and the strong electron-withdrawing effect of the fluorine substituents. 1,3-Dicyanohexafluorobicyclo[1.1.1]pentane (1,3-$(CN)_2$-**2**) was synthesized from hexafluorobicyclo[1.1.1]pentane-1,3-carboxamide (1,3-$(CONH_2)_2$-**2**), which was prepared from 1,3-$(COOH)_2$-**2**.[30]

Attempts to synthesize 1,3-difluorobicyclopentane (1,3-F_2-**1**) by treatment of either bicyclo[1.1.1]pentane-1,3-dicarboxylic acid[31] or 1-fluorobicyclo[1.1.1]pentane-3-carboxylic acid[32] with xenon difluoride were unsuccessful,[27] as were several attempts to produce 1,3-F_2-**1** by fluorination with diethylaminosulfur trifluoride[33] of bicyclo[1.1.1]pentane-1,3-diol, obtained by Baeyer–Villiger oxidation of the corresponding diacetyl derivative followed by alkaline hydrolysis of the resulting diester.[34,35] Attempted preparation of perfluorobicyclo[1.1.1]pentane (1,3-F_2-**2**) either by reaction of 1,3-$(COOH)_2$-**2**[30] with xenon difluoride or by fluorination of **2** with elemental fluorine or with potassium hexafluoronickelate(IV) failed as well.

CHEMISTRY
AN ASIAN JOURNAL

Calculated Molecular Structure

Figure 1 shows the bicyclopentane structure and the labels of atoms (C_a, C_b) and directions (σ, π) with respect to the threefold axis. In the ground state, the C_b–C_b distances in the parent 1,3-Y_2-**1** are about 0.1 Å shorter than in the perfluorinated 1,3-Y_2-**2**, and the C_a–C_a distances in 1,3-Y_2-**1** are about 0.05 Å longer than in 1,3-Y_2-**2**. The optimized geometries of the neutral 1,3-Y_2-**1** and 1,3-Y_2-**2** molecules are summarized in Table 1.

Table 1. MP2-optimized equilibrium structures of the ground state for 1,3-Y_2-**1** and 1,3-Y_2-**2** (Y = H, F, Cl, Br, I, At, CN).[a]

Molecule	C_b–C_b	C_a–C_a	C_b–C_a	C_b–Y	C_a–X
C_5H_8	1.882	2.142	1.554	1.093	1.095
C_5F_8	1.915	2.130	1.559	1.330	1.339
$C_5H_6F_2$	1.806	2.173	1.545	1.353	1.092
$C_5F_6H_2$	1.970	2.088	1.557	1.089	1.345
$C_5H_6Cl_2$	1.820	2.165	1.546	1.751	1.092
$C_5F_6Cl_2$	1.935	2.120	1.560	1.714	1.336
$C_5H_6Br_2$	1.820	2.167	1.547	1.910	1.092
$C_5F_6Br_2$	1.938	2.119	1.561	1.873	1.336
$C_5H_6I_2$	1.821	2.170	1.549	2.130	1.092
$C_5F_6I_2$	1.941	2.117	1.561	2.088	1.335
$C_5H_6At_2$	1.778	2.186	1.544	2.356	1.091
$C_5F_6At_2$	1.917	2.128	1.558	2.300	1.335
$C_5H_6(CN)_2$	1.875	2.155	1.558	1.443	1.093 (CN: 1.177)
$C_5F_6(CN)_2$	1.971	2.116	1.569	1.432	1.333 (CN: 1.177)

[a] Bond lengths in Å.

Spin–Orbit Coupling

To estimate the accuracy of the present spin–orbit calculations, the spin–orbit splitting between the $^2P_{1/2}$ and $^2P_{3/2}$ states of the halogen atoms was calculated in the same way (Table 2). The experimental spin–orbit splitting was well-reproduced for the F and Cl atoms, but the calculated value was too small for Br, I, and At.[36] This underestimation of the splitting is due to the use of a contracted basis set with a relativistic effective core potential (RECP) and to the approximations used in the calculations as described in the Experimental Section.

Table 2. The $^2P_{1/2}$–$^2P_{3/2}$ spin–orbit splitting (cm^{-1}) for halogen atoms calculated with the basis set used for 1,3-Y_2-**1** and 1,3-Y_2-**2**.

Atom	Experimental[a]	Calculated
F	404	470
Cl	881	830
Br	3685	2870
I	7603	6200
At	22155[b]	17940

[a] C. E. Moore, *Atomic Energy Levels*, *Vol. 1–3*, National Bureau of Standards, U.S. Government Printing Office, Washington, D.C., **1971**. [b] Calculated.[36]

Photoelectron Spectra

1,3-Y_2-**1**: In Figures 2–7, we compare the observed He(I) PES of 1,3-Y_2-**1** with those calculated by the SAC-CI method with and without spin–orbit coupling. For Y = F and At, only the calculated results are available (Figure 3). Figure 8 compares the valence ionized states calculated by the SAC-CI method for **1** and its five 1,3-dihalo derivatives up to 20 eV. Tables summarizing the calculated ionization potentials (IPs), monopole intensities, ionization characters, and experimental values of 1,3-Y_2-**1** and an additional compound, 1,3-Br_2-2,2-Cl_2-**1**, are given in the Supporting Information. For convenience, in all figures the ionized states are labeled by symbols appropriate for the D_{3h} point group, although the ions should be described by the spin-double group when spin–orbit interaction is included. Molecular-orbital (MO) numbering is from the highest down to relate the MOs directly to the ionized states.

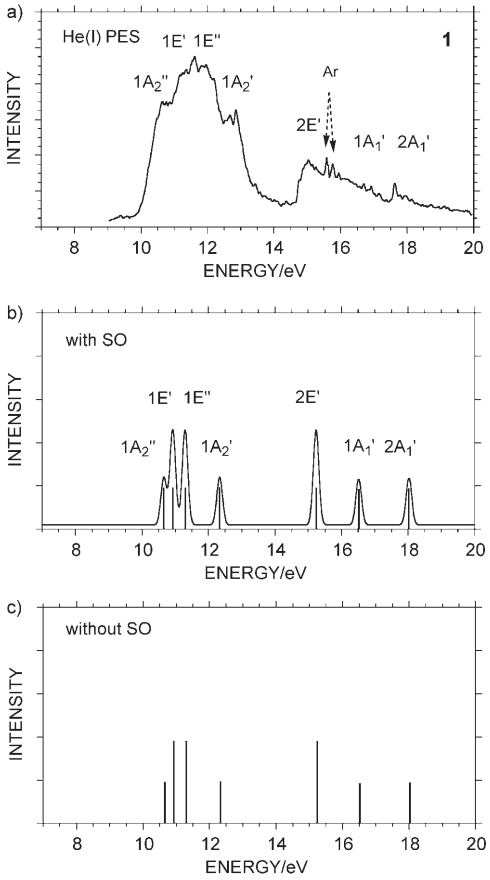

Figure 2. He(I) PE and SAC-CI spectra with and without the inclusion of spin–orbit (SO) interaction for **1**.

Figure 9 displays the form of the MOs of **1**, and Figure 10 compares the optimized ground-state and ionized-state geometries of 1,3-Cl_2-**1** and 1,3-Br_2-**1**.

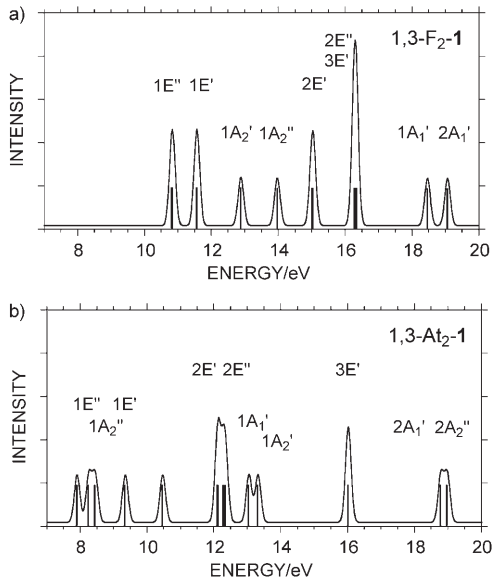

Figure 3. SAC-CI spectra of 1,3-F_2-**1** and 1,3-At_2-**1** with the inclusion of spin–orbit interaction.

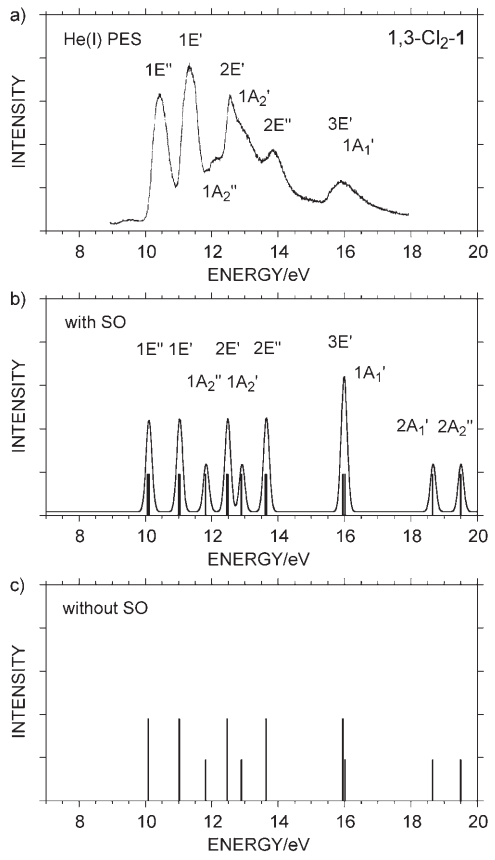

Figure 4. He(I) PE and SAC-CI spectra with and without the inclusion of spin–orbit interaction for 1,3-Cl_2-**1**.

1,3-Y_2-**2**: Figure 11 shows the observed He(I) PE spectra of 1,3-Y_2-**2**, except for the cases Y = F, Cl, and At for which only the calculated results are available (Figure 11 b, c, g).

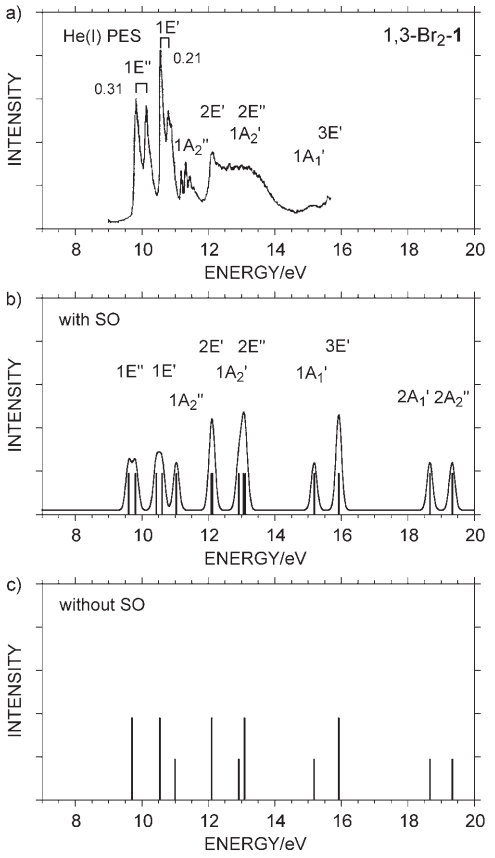

Figure 5. He(I) PE and SAC-CI spectra with and without the inclusion of spin–orbit interaction for 1,3-Br_2-**1**.

The valence ionized states calculated by the SAC-CI method for **1**, **2**, and the five 1,3-dihalo derivatives of **2** are compared in Figure 12. The calculated IPs, monopole intensities, and ionization characters of 1,3-Y_2-**2** are compared with the experimental values in tables included in the Supporting Information.

Koopmans' Theorem and Correlation Diagrams

The tables in the Supporting Information show that the vertical ionization energies deduced from the Koopmans' theorem are far from numerical agreement with the measured values, whereas the SAC-CI results agree very well. Nevertheless, there is a one-to-one correspondence between the Koopmans' and the more accurate SAC-CI description, such that the ionized states predicted by the latter can be well described by stating from which MO an electron is being removed. This permits the use of MO correlation diagrams of the type used so successfully for similar compounds by Heilbronner and co-workers[16,17] instead of state correlation diagrams, thus greatly simplifying the following discussion. Figures 13 and 14 show the correlation of the important MOs associated with the ionized states through the Koopmans' theorem.

CHEMISTRY
AN ASIAN JOURNAL

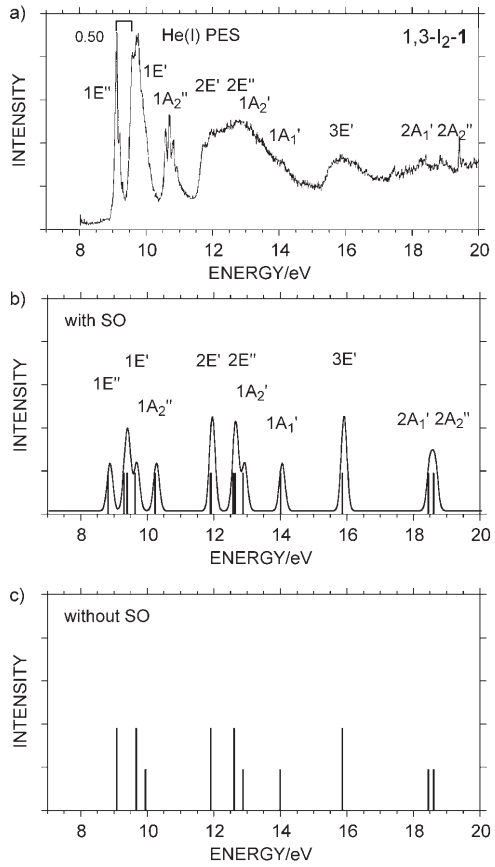

Figure 6. He(I) PE and SAC-CI spectra with and without the inclusion of spin–orbit interaction for 1,3-I_2-**1**.

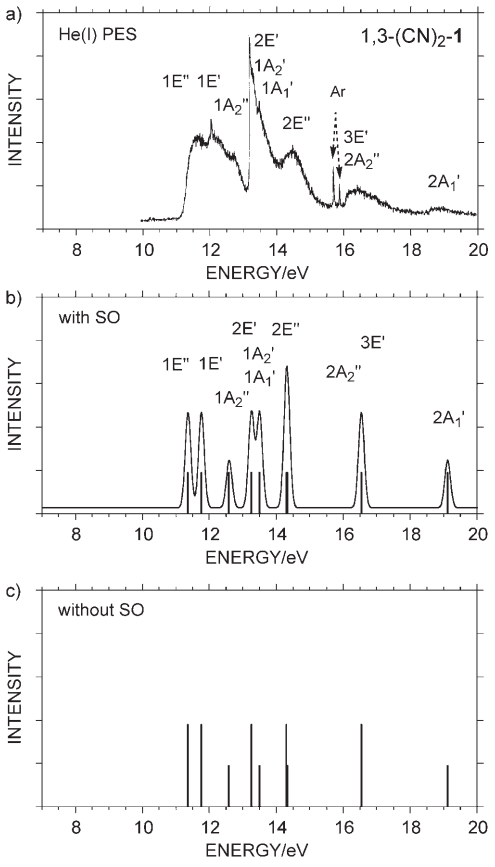

Figure 7. He(I) PE and SAC-CI spectra with and without the inclusion of spin–orbit interaction for 1,3-$(CN)_2$-**1**.

Discussion

Synthesis

Our inability to prepare 1,3-F_2-**1** and 1,3-F_2-**2** is disappointing, but as we shall see below, the general agreement of the calculated and observed PES is so good that the computational results for these two compounds may be taken as confident predictions of their PES and used for the analysis of trends in place of the latter.

Photoelectron Spectra

1,3-Y_2-**1**: We describe first the valence ionized states of the parent molecule **1**. Figure 9a–c shows 11 of its 14 occupied valence MOs (only one member of each degenerate pair is shown) without the innermost e′ and a′ MOs, whose IPs are higher than 20 eV and lie outside our experimental range. The valence MOs are described by linear combinations of two C_b–H, six C_a–H, and six C_a–C_b bonding MOs. As originally assigned by Gleiter et al.[14] on qualitative grounds, the $1A_2''$ and $1A_1'$ states are produced by ionization from the out-of-phase ($1a_2''$) and in-phase ($1a_1'$) combinations of C_b–H bond orbitals, respectively, and the splitting of these two states was both calculated and measured to be 5.9 eV. This splitting can be viewed as being caused by a combination of direct transannular interaction between the C_b–H bonds and the differential interaction of their out-of-phase and in-phase combinations with the appropriate symmetry orbitals of the bicyclic cage. The 1E′ and 1E″ states are due to ionization from the 1e′ and 1e″ MOs formed from the C_a–C_b

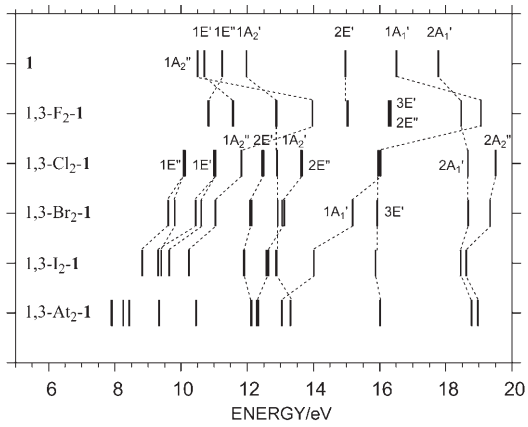

Figure 8. Valence ionized states of 1,3-Y_2-**1** (Y = H, F, Cl, Br, I, At) calculated by the SAC-CI method.

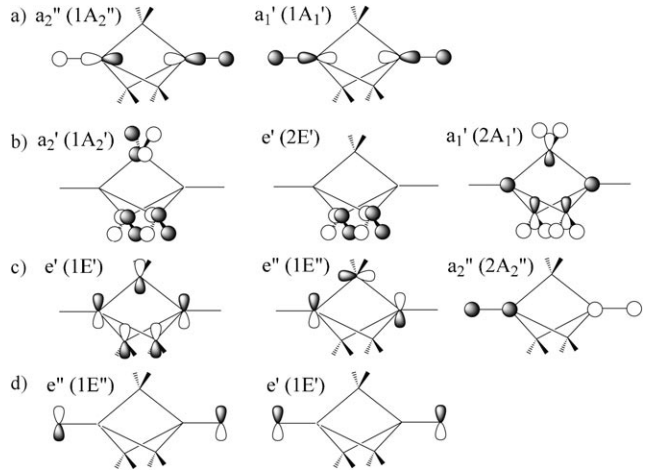

Figure 9. a) C_b–H, b) C_a–H, and c) C_a-C_b bonding MOs of C_5H_8. d) The outermost e″ and e′ MOs of 1,3-Y_2-**1** (Y = halogen).

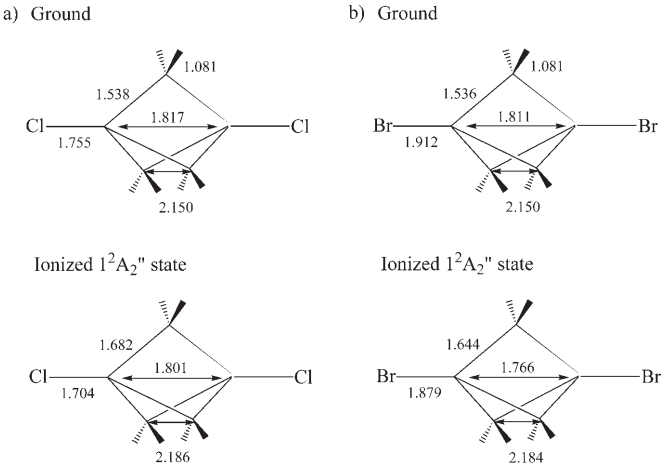

Figure 10. Equilibrium structures of the ground and ionized $1^2A_2''$ states of a) 1,3-Cl_2-**1** and b) 1,3-Br_2-**1**. Bond lengths and distances are given in Å.

bond orbitals, whereas the $1A_2'$, 2E′, and $2A_1'$ states are attributed to ionization from the $1a_2'$, 2e′, and $2a_1'$ MOs formed from the C_a–H bonds.

Next, the effects of the axially symmetric bridgehead substituents Y are considered in Figures 13 and 14, patterned after the work of Heilbronner and co-workers[16,17] (experimental data have been used except for Y = F). Three types of lines are used in Figure 13 to indicate the full details of the orbital correlations for Y = I: dashed lines for σ-symmetry and full lines for π-symmetry orbitals at the bridgeheads, and dotted lines for orbitals of other types. Figure 14 shows only the correlations for π-symmetry orbitals at the bridgeheads (i.e., full lines) for other choices of Y for simplicity.

In the conversion of **1** into 1,3-Y_2-**1**, each Y substituent provides four valence orbitals in place of the one for the hydrogen atom, thus expanding the overall size of the valence space. In the correlation diagrams, we consider the effect of both π-symmetry atomic orbitals (AOs) present on each Y, but we include only one of the two that are of σ symmetry (the other is mostly of s character and too low in energy to be important). When Y = CN, we consider all four triple-bond orbitals of each substituent that are of π symmetry, and again only one of those of σ symmetry.

With these simplifications, the conversion of **1** into 1,3-Y_2-**1** introduces two significant changes. First, the σ-symmetry C_b–H bonds are replaced with σ-symmetry C_b–Y bonds. Second, the two π-symmetry AOs on Y (or π-bond orbitals in 1,3-$(CN)_2$-**1**), which are absent in the valence shell of H, interact with the MOs of the cage. The former describes the valence-space size-conserving σ effect (the inductive I effect) and the latter, the valence-space size-expanding π effect (the hyperconjugative E effect) of the substituent. As described by Gleiter et al.,[14] the lowest 1E″ and 1E′ states are due to the ionizations from the pπ MOs 1e″ and 1e′ that are largely located on the bridgehead halogen atoms and contain the out-of-phase and in-phase combinations of their lone-pair AOs, respectively (Figure 9d). The only exception is the case Y = F, owing to the very low energy of the fluorine lone-pair orbitals. In 1,3-F_2-**1**, fluorine lone-pair character resides in the MOs 3e′ and 2e″, whereas hardly any is contained in the MOs 1e′ and 1e″. In 1,3-F_2-**2**, only 1e′ has significant F lone-pair character; 1e″ again does not.

We consider the σ effect first, with Y = I as an example (Figure 13). The energy of a truly isolated C–Y σ-bond orbital, approximated from the PES of CH_3Y, is shown in the central column. As this energy is different from that of the C–H bond, the interactions with the cage orbitals are different, too. The resulting pair of C_b–Y bond orbitals $1a_1'$ and $1a_2''$ is split by less than the 5.9 eV found for C_b–H (calculated (eV) for Y = F: 5.6; Cl: 4.2; Br: 4.2; I: 4.0; At: 4.0). The case of 1,3-$(CN)_2$-**1** is complicated by the presence of nitrogen lone-pair orbitals, which are also of σ symmetry but are being ignored in the discussion of orbital correlations. They introduce two relatively high energy orbitals calculated to be split by 0.9 eV.

Next, we turn to the π effect, which increases the total number of valence orbitals in the correlation diagrams by four. In Figures 13 and 14 , the new pairs of degenerate p orbitals on Y, shown in the central column, are of e′ and e″ symmetry. The energies shown are those measured for CH_3Y[37] and corrected[15] for the effect of hyperconjugation with the methyl group. These orbitals interact with the 1e′ and 1e″ orbitals already present in the bicyclic cage and endowed with large amplitudes on the p_x and p_y AOs on C_b. The resulting difference in orbital energies in 1,3-Y_2-**1** is always larger for the antisymmetric e″ orbitals (calculated (eV) for Y = F: 5.5; Cl: 3.5; Br: 3.4; I: 3.5; At: 3.6; CN: 2.9) than for the symmetric e′ orbitals (calculated (eV) for Y = F: 3.0; Cl: 1.5; Br: 1.6; I: 2.2; At: 3.1; CN: 1.5). The difference is especially large for Y = F, not because the orbital interaction is particularly strong, but because the energies of the interacting levels are far apart.

If we consider the simplest possible interpretation, with only the 1e′ or 1e″ orbitals of the cage and the π-symmetry lone-pair orbitals of the halogens (Figure 14), we find that

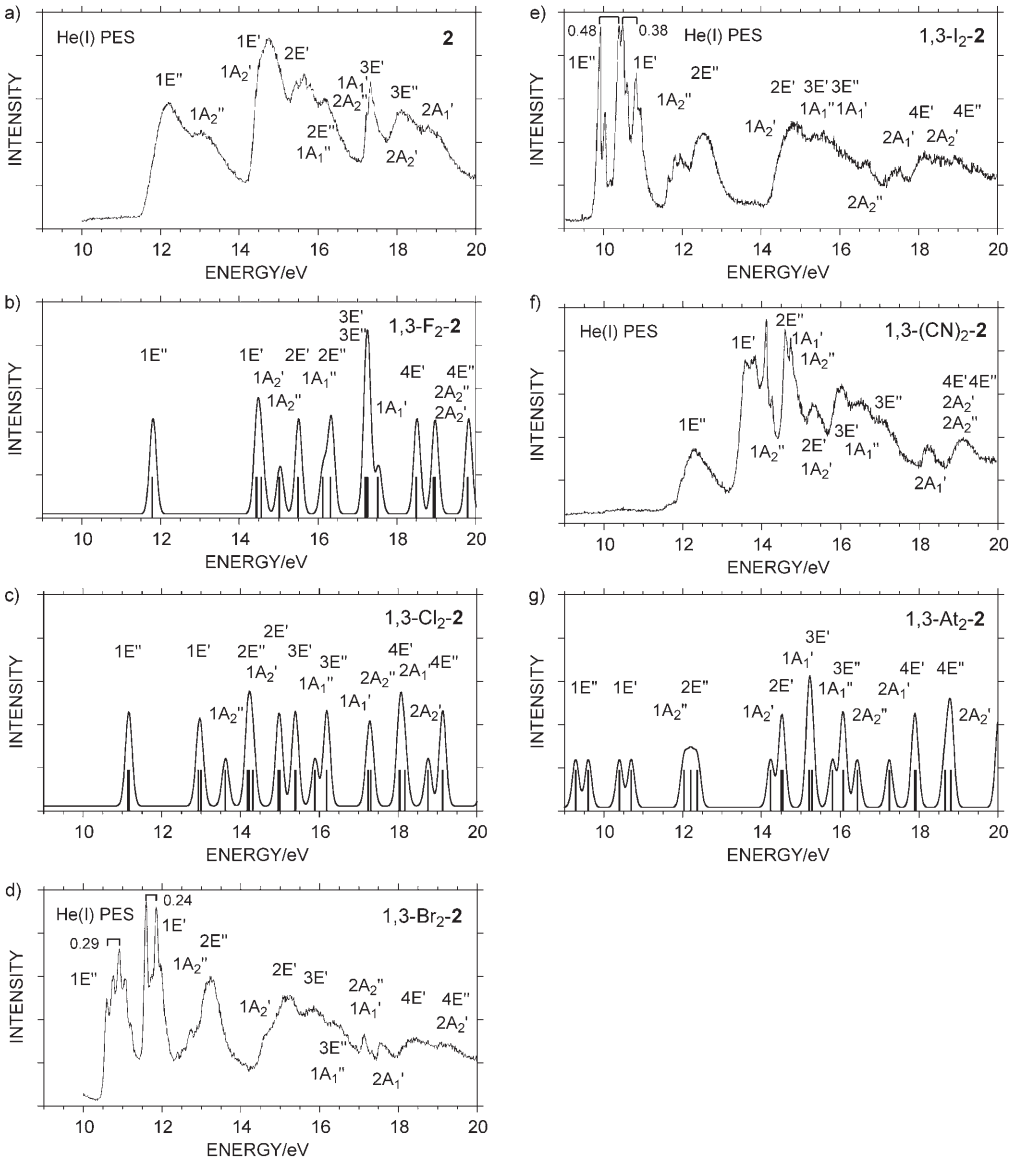

Figure 11. He(I) PES of 1,3-Y_2-**2** (Y = H, F, Cl, Br, I, CN, At). All spectra were experimentally obtained except those of Y = F, Cl, and At, which are SAC-CI spectra with the inclusion of spin–orbit interaction.

the effective interaction ("resonance") integral between the cage orbital and the halogen orbital is of the order of 0.75 eV for the e′ orbitals and about twice as large for the e″ orbitals (its magnitude decreases with increasing atomic number of the halogen). This simplest description works best if it is assumed that the e′ and e″ orbital assignment of the close-lying MOs of **1** needs to be interchanged relative to the computational results shown in the drawings. As the energies of these two orbitals are very similar, it is quite conceivable that the computed order may be in error. The difference between the effective interaction integrals for the two cage MOs suggests that the amplitude of the 1e′ orbital at C_b is only about half that of the 1e″ orbital. Indeed, on the basis of Weinhold's natural atomic orbitals (NAOs),[38] the coefficient of the self-consistent field (SCF) 1e′ MO of **1** calculated presently on the π-symmetry $C_b(p_x)$ and $C_b(p_y)$ valence orbitals is 0.32, whereas that of the 1e″ MO of **1** is 0.50 (HF/D95). This is not surprising given that 1e″ has a node passing through all three bridge carbon atoms, which pushes its amplitude towards the bridgeheads.

Turning now to the individual compounds, we note that the $1a_2''$ and $2a_1'$ orbitals are at lower energy in 1,3-F_2-**1** than the corresponding $1a_2''$ and $1a_1'$ orbitals in **1**, and that their splitting is decreased from 6.0 to 5.1 eV. New 2e″ and 3e′ orbitals associated with the pπ MOs of the terminal F atoms appeared at about 16.3 eV, close to the first IP of the F atom (17.42 eV), and these would need to be considered if one wished to evaluate lone-pair interactions mediated by the cage. As seen in Figures 8 and 14, other states, 1E″, 1E′, $1A_2'$, 2E′, and $1A_1'$ (note that state $1A_1'$ in 1,3-F_2-**1** corre-

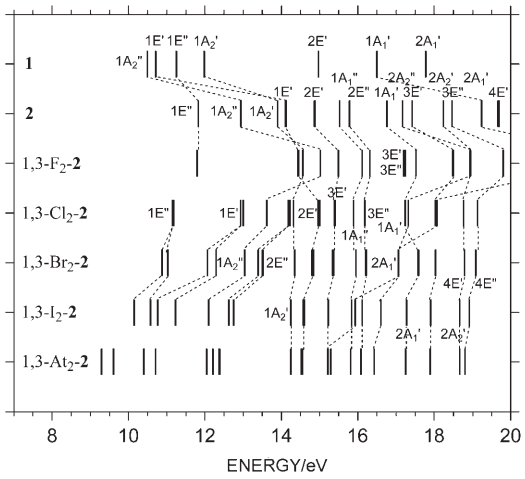

Figure 12. Valence ionized states of 1,3-Y_2-**2** (Y = H, F, Cl, Br, I, At) calculated by the SAC-CI method.

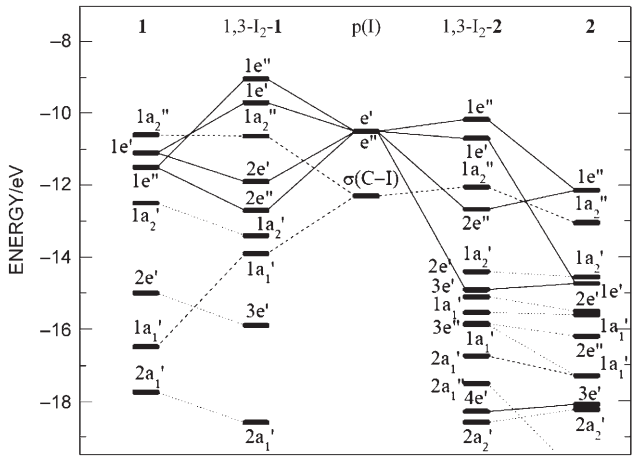

Figure 13. Correlation of measured ionization energies and their assignment to MOs. Center: lone-pair AOs on I and the C–I bond orbitals; first and fifth columns: MOs of cages **1** and **2**; second and fourth columns: MOs of 1,3-I_2-**1** and 1,3-I_2-**2**. For the definition of line types, see text.

sponds to state $2A_1'$ in **1**), are less influenced by F substitution, as they correspond to ionizations from the C_a–C_b or C_a–H bond orbitals.

The effects of the conversion of **1** into the other dihalo derivatives 1,3-Y_2-**1** (Y = Cl, Br, and I) are very similar, as seen from Figures 8, 13, and 14. The resulting new E′ and E″ states associated with the π MOs of the terminal halogen atoms become less strongly bound as the atomic number of Y increases. The spin–orbit splitting in the Br and I derivatives is prominent in the 1E′ and 1E″ states, which are primarily due to ionizations from the pπ MOs of the terminal halogens Y, but not in the 2E′ and 2E″ states, which have a smaller amplitude on the halogen atoms. In the PES of 1,3-Br_2-**1**, two pairs of split peaks were observed and are attributed to the 1E′ and 1E″ states. The first peak in the PES of 1,3-I_2-**1** is assigned to one component of the spin–orbit state of 1E″ and the second peak to its other component, which overlaps with both weakly split spin–orbit components of 1E′.

The third band in the experimental spectra, assigned to the $1A_2''$ state, has vibrational structure for Y = Br or I, which indicates a significant change in geometry along the direction of one of the normal modes upon ionization. The equilibrium molecular structures of the ground and $1A_2''$ states of 1,3-Y_2-**1** (Y = Cl, Br) calculated by the UHF/6-31G(d) method are shown in Figure 10. The C_b–C_b distance in 1,3-Y_2-**1** (Y = Br, I) was calculated to shrink upon ionization from the a_2'' MO, which is antibonding with respect to the C_b–C_b interaction, and we assign this as the cause of the vibrational structure. The calculated geometrical change is less pronounced for 1,3-Cl_2-**1**, which may be the reason why the vibrational structure is missing in its spectrum. The fourth band, from 12.0 to 14.0 eV, is attributed to the 2E′, $1A_2'$, and 2E″ states.

As already noted, the $1A_2''$ state of 1,3-I_2-**1** exhibits vibrational structure, similarly as it did in 1,3-Br_2-**1**. The overlapping bands at 12–14 eV are attributed to the 2E′, 2E″, $1A_2'$, and $1A_1'$ states. The 3E′ state is assigned to the band at about 16.0 eV, and the $2A_1'$ and $1A_2''$ states to the band near 18.0 eV.

The SAC-CI general-*R* method, which describes shake-up states more accurately, was also used for 1,3-I_2-**1**. The main peaks lower than 16 eV were not influenced much, whereas many correlation peaks appeared in the energy region 16–18 eV. These states have distributed intensities due to the final-state correlation interactions with the 3E′, $2A_1'$, and

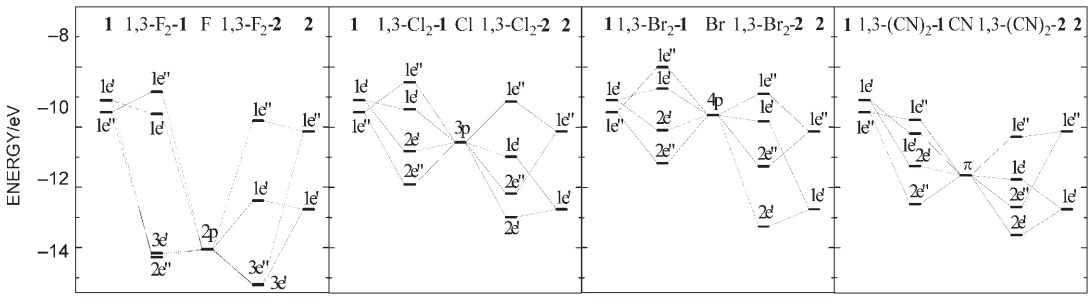

Figure 14. Correlation of selected ionization energies and their assignment to MOs for 1,3-Y_2-**1** and 1,3-Y_2-**2** (calculated for Y = F and measured for Y = Cl, Br, and I).

$2A_2''$ states. This result further indicates that the valence ionized states of 1,3-Y_2-**1** can be assigned by the SD-*R* method.

In 1,3-At_2-**1**, the calculated spin–orbit interaction is quite large in the five energetically low-lying states, 1E′, 1E″, and $1A_2''$. The 2E″ and $1A_1'$ states are stabilized by At substitution, whereas the IPs of the 2E′, $1A_2'$, 3E′, $2A_1'$, and $2A_2''$ states are almost constant in 1,3-Y_2-**1** regardless of Y.

The IPs of the $1A_2''$, 2E′, and $2A_1'$ states of 1,3-$(CN)_2$-**1** do not differ much from those of the other derivatives, as these states result from ionizations from the C_a–H bonding MOs. However, the Y = CN substitution influences the C_b–Y and C_a–C_b bonding MOs and thus changes the corresponding IPs. For Y = CN, the cage-mediated π interaction was calculated to be 0.40 eV and observed to be 0.45 eV, smaller than for the halogen derivatives. The difference can be attributed to the relatively small amplitude of the π_{CN} orbitals on carbon, due to their polarization toward nitrogen, and to the presence of relatively low energy π_{CN}* orbitals with a larger amplitude on carbon. Many valence ionized states are present in the 11–15-eV region.

1,3-Y_2-**2**: Next, we turn to the effects of hexafluorination and compare the ionization spectrum of **2** with that of **1**. As expected, most MOs of the hexafluorinated cage are at much lower energies. The bonds formed by the F(pπ) AOs (see Figure 1 for definitions) are strongly polarized toward the electronegative fluorine substituent, which accounts for its +I effect. They act on the symmetric MOs of the cage and are incapable of interacting with its antisymmetric MOs such as 1e″. In fact, the IP of the 1E″ state hardly changes upon F substitution, as antisymmetric cage MOs such as 1e″ are influenced by the F(pσ)–C_a(pσ) antibonding interaction (−E substituent effect). The energy splitting of the $1A_2''$ and $2A_1'$ states, produced by the ionizations from the C_b–H bonding MOs, is about 6.5 eV, slightly larger than in **1**. Many valence states due to ionization from fluorine lone-pair orbitals appear in the 15–20-eV region.

The general considerations of bridgehead-substituent effects for **2** are the same as for **1**. The increased bridgehead–bridgehead separation in the hexafluorinated 1,3-Y_2-**2** relative to the parent 1,3-Y_2-**1** was already known[30] and follows from Bent's rules[39] and the high electronegativity of fluorine. The C_b–Y bond lengths reflect the sizes of the halogen atoms in a regular fashion, and the separation of the bridgehead halogens Y in 1,3-Y_2-**2** is thus larger than in 1,3-Y_2-**1**. Nevertheless, we shall see below that the lone–pair orbital splitting caused by the cage-mediated interaction of the bridgehead substituents is actually larger.

In the calculated spectra of 1,3-F_2-**2**, all the valence states except for 1E″ are more strongly bound than those of **2**, especially those resulting from ionization from the C_b–F bond orbitals a_2'' and a_1'. In consequence, the 1E″ state at about 10.8 eV is separated from the other states, and the corresponding peak becomes quite isolated. The 3E″ and 3E′ states appear at about 17.0 eV. As in 1,3-F_2-**1**, the 1E″ state hardly involves fluorine lone-pair orbitals at all due to symmetry, but, in contrast to 1,3-F_2-**1**, the 1E′ state of 1,3-F_2-**2** does. This can be viewed as a result of the great stabilization of the 1e′ MO by the six fluorine substituents.

The spectra of 1,3-Y_2-**2** (Y = Cl, Br, I) are similar. In comparison with those of 1,3-Y_2-**1** (Y = Cl, Br, I), the σ-symmetry $1A_2''$ and $2A_1'$ states are more strongly bound by 2.0–2.5 eV, and the energy splitting between these states was calculated to be 4.6, 4.6, and 3.9 eV for Y = Cl, Br, and I, respectively. The π-symmetry 1E″ and 1E′ states are also more strongly bound, by 1.1, 1.3, and 1.3 eV for Y = Cl, Br, and I, respectively. The calculated energy splitting of these two states was increased to 1.8 (Cl), 1.2 (Br), and 0.7 eV (I), and the measured values were 0.86 (Br) and 0.58 eV (I). In 1,3-Y_2-**1**, this splitting was 0.9 (Cl), 0.8 (Br), and 0.6 eV (I), and the experimental results were 0.90, 0.72, and 0.66 eV, respectively. The splitting for 1,3-Br_2-**1** and 1,3-$(C_2H)_2$-**1** (diethynyl) was measured previously[14] to be 0.72 and 0.68 eV, respectively. The increased splitting of the 1e′ and 1e″ orbitals in 1,3-Cl_2-**2** compared to 1,3-Cl_2-**1** is particularly remarkable, and we discuss its origin below.

Factors Determining the Strength of Through-Cage π Interactions

As the lone-pair orbitals on substituents located at the bridgeheads of a cage (or other π-symmetry orbitals located on bridgehead substituents) are too far apart for significant direct interaction, it is their interaction with the cage orbitals that dictates the strength of the cage-mediated interaction. The standard measure of the strength of this interaction is half the difference between the energies of the MOs that contain large symmetric and antisymmetric contributions from the lone-pair orbitals.[2] This is entirely analogous to the usual use of the difference of the π-bonding and π*-antibonding orbital energies as a measure of the strength of the π interaction when such orbitals overlap and interact directly. It is justified in the two-state approximation, when Y^+–cage–Y and Y–cage–Y^+ are the only states that need to be considered.[5,6,8] This requires the energies of the relevant orbitals on the substituents Y to be well removed from those of the MOs of the cage, such that the substituent orbitals do not delocalize into the cage. In most commonly used cages and substituents Y, this condition is not very well fulfilled. If it were, there would be no through-bond coupling.

In the simplest case of through-bond coupling,[3] the situation is simplified in that only one vacant antisymmetric and one occupied symmetric orbital of the mediator need to be considered. This is not our case. As the energies of the halogen lone-pair AOs are comparable to those of the 1e′ and 1e″ MOs of the parent cage **1** (Y = Cl, Br, I), their mutual interaction is primary. Either of the resulting MO pairs of the substituted cage, 1e′/1e″ or 2e′/2e″, could be used for the evaluation of the cage-mediated interaction, as both pairs contain comparable amounts of halogen lone-pair character. Inspection of Figures 13 and 14 shows that roughly similar results would be obtained. It is customary[14] to use the higher-energy pair 1e′/1e″, for which more reliable experimental values can usually be secured, and we shall follow

this practice. In **2**, the energies of the 1e′ cage MO actually lie well below those of the halogen lone-pair orbitals, thus further justifying the use of the 1e′/1e″ pair.

The splitting of the π-symmetry orbitals in 1,3-Y_2-**1** is large: 0.9 (Cl), 0.8 (Br), and 0.6 eV (I); it is even larger in 1,3-Y_2-**2**: 1.8 (Cl), 1.2 (Br), and 0.7 eV (I) (calculated values). For comparison, in bicyclo[2.2.2]octane substituted with bridgehead halogens,[16] in which the lowest 1E″ and 1E′ states are also due to ionizations from the halogen lone-pair orbitals, the splitting is only 0.14 eV for Br substituents. For Cl substituents, the splitting cannot be much larger, but its exact value is unclear due to unresolved bands. In 1,4-disubstituted cubane,[17] the splitting between the analogous states of E_u and E_g symmetry is only 0.4 (Cl), 0.25 (Br), and 0.36 eV (I). In this regard, the bicyclo[1.1.1]pentane cage, especially its hexafluorinated version, is unique.

When would cage-mediated π interactions defined in this fashion be strong? If the symmetric combination of substituent π orbitals interacted with the symmetric cage orbital(s) exactly as much as their antisymmetric combination interacts with the antisymmetric cage orbital(s), and if the symmetric and antisymmetric MOs of the parent cage had the same energies, the energies of the symmetric and antisymmetric upper MOs resulting from these interactions would be equal, and the through-cage interaction would be said to vanish. Clearly, one of the factors that dictate the cage-mediated interaction, as it is usually defined, is the difference between the ability of the symmetric and antisymmetric occupied cage orbitals to interact with substituent orbitals. In the simplest possible description, only one cage MO of each symmetry needs to be considered, and this is the case in the first approximation for the e′ (symmetric) and e″ (antisymmetric) MOs of **1** and **2**, both of which are bonding and occupied.

In reality, the symmetric and antisymmetric MOs of a cage will hardly ever have the same energy. Their energy difference represents a second factor that dictates the energy difference of the highest-energy symmetric and antisymmetric combinations of the initially degenerate halogen lone-pair orbitals that result from mixing with cage orbitals (Figures 13 and 14). In other words, the important factors are the difference between the diagonal elements and the difference between the off-diagonal elements of the 2×2 matrices that describe the interactions in the symmetric and antisymmetric cases.

The two factors, diagonal and off-diagonal, change independently from cage to cage. One or the other can dominate, or both could be important and might interfere with each other. This is exemplified by the nearly exact degeneracy of the 3e′ and 3e″ MOs of 1,3-F_2-**2** (Figure 14), in which the latter is favored by the off-diagonal interaction but disfavored by the diagonal one.

The parent cage **1** (Y = Cl, Br, I) provides an example of off-diagonal dominance. The energies of the starting 1e′ and 1e″ orbitals of the cage are nearly identical, and it is the difference in their effective interaction integrals with the lone-pair orbitals that dominates the final 1e′–1e″ separation in the substituted cage. To the first order, these effective resonance integrals are proportional to the amplitudes of the e′ and e″ cage orbitals at the bridgeheads. As we saw above, the amplitude is larger for the e″ orbitals by a factor of about two (0.50 vs. 0.32 at the HF/D95 level of calculation, in which the e′ and e″ orbitals are degenerate at −12.46 eV), and the final e″ orbital ends up lying above the final e′. One of the other well-studied highly symmetric cages, cubane,[17] is also off-diagonally dominated and has a significant but smaller difference in the bridgehead amplitudes of the symmetric (e_u) and antisymmetric (e_g) cage MOs, which are again close in energy. The former lies at −10.6 eV, and its amplitude at the bridgehead natural valence p orbital is 0.28 at the HF/D95 level. The latter is at −10.8 eV, and the amplitude is 0.43. The other, bicyclo[2.2.2]octane,[16] is diagonally dominated. At the optimized staggered geometry, the symmetric *e* MO of the cage lies at −13.34 eV, and its amplitude at the bridgehead is 0.35, whereas the antisymmetric *e* orbital is located at −10.94 eV, and its amplitude at the bridgehead is nearly the same at 0.34 (HF/D95).

In 1,3-F_2-**1**, the splitting of the MOs that carry fluorine lone-pair character, 3e′ and 2e″, nearly vanishes as a result of interactions among several orbitals.

The differences in orbital-energy splitting for the Cl, Br, and I substituents reflect the differences in the carbon–halogen π resonance integrals and the differences in the relative energies of their lone-pair orbitals compared with those of the e′ and e″ MOs of the cage. The relative strength of the cage-mediated halogen–halogen interaction is not a one-dimensional property and could depend on the choice of halogen. It seems that the magnitude of the carbon–halogen π resonance integrals is the dominant factor, such that the strength of the coupling always decreases in the order Cl > Br > I.

The hexafluorinated cage **2** (Y = Cl, Br, I) provides an example of diagonal dominance. The energies of the 1e′ and 1e″ MOs of the parent cage are vastly different. The former is more stable by 2.59 eV and hardly interacts with the halogen substituent lone-pair orbitals at all, whereas 1e″ interacts roughly as much as in **1**. As a result, the energy of the final e″ orbital ends up being significantly greater than that of the final e′ orbital. Therefore, the cage-mediated interaction is much stronger in **2** than in **1**. In 1,3-F_2-**2**, the diagonal and off-diagonal effects conspire to give near-exact degeneracy for the 3e′/3e″ MO pair and, hence, no cage-mediated coupling of the halogen π lone-pairs at all. This was also the outcome in 1,3-F_2-**1**, albeit for a different reason. Both of these cases illustrate that the relative ability of a cage to mediate electronic interactions between substituents is not only a function of cage structure, but also of the nature of the substituent.

Use of Orbital-Energy Splitting as a Measure of Through-Cage Interaction

We have just seen that the usual measure of through-cage interaction, the difference in the energies of the symmetric

CHEMISTRY
AN ASIAN JOURNAL

and antisymmetric MOs of the final system that has large contributions from substituent orbitals (for Y = Cl, Br, and I, 1e′ and 1e″ in **1** and **2**), contains contributions from both off-diagonal and diagonal effects as defined above. As we are not really dealing with a two-state system, the strength of the interaction between the Y^+–cage–Y and Y–cage–Y^+ states need not be simply related to the orbital splitting measured. It is thus doubtful that the diagonal and off-diagonal effects could enter on equal footing when one considers all other properties of interest, such as the ease of charge transfer through the cage. After all, although in a homonuclear diatomic molecule the splitting of the symmetric and antisymmetric MOs that result from the interaction of AOs is a good measure of its strength, in a heteronuclear diatomic this is not so, and in a limiting case, the splitting is merely a measure of the difference in electronegativity between two weakly interacting partners, not a measure of the strength of their interaction. A more complicated analysis is called for, but lies outside the scope of this paper.

Conclusions

We have studied the valence ionized states of a series of bicyclo[1.1.1]pentane derivatives, 1,3-Y_2-**1** (Y = H, Cl, Br, I, CN) and 1,3-Y_2-**2** (Y = H, Br, I, CN), with He(I) photoelectron spectroscopy and the SAC-CI method, including spin–orbit coupling. The calculated spectra agree well with those observed, thus allowing quantitative assignments. The spin–orbit interactions are predicted to be especially large in the five lowest ionized states of 1,3-At_2-**1** and 1,3-At_2-**2**.

When estimated by the standard procedures, the cage-mediated interactions between bridgehead substituents are unusually large, especially in the hexafluoro derivatives 1,3-Y_2-**2** (Y = Cl, Br, I). We have analyzed the origin of this strong interaction in simple terms and identified the two primary contributing factors: 1) the difference in the bridgehead amplitudes of the symmetric and antisymmetric cage MOs responsible for the interaction and the strength of the resonance integral between the bridgehead carbon atom and the substituent (the off-diagonal factor), and 2) the difference in the energies of these MOs (the diagonal factor). In general, off-diagonal coupling is maximized when the amplitudes of the symmetric and antisymmetric cage MOs on the bridgeheads are very different and the C_b–Y resonance integrals are large, whereas diagonal coupling is favored when one of these cage MOs interacts very weakly with the substituent orbitals because of a large energy gap. However, it is not obvious that there is a simple relation between the total orbital-energy splitting normally taken as a measure of cage-mediated interaction and other properties that depend on such interaction, and we suspect that, for some properties, only the off-diagonal coupling counts. We do not trust the conclusion suggested by a superficial look at the present results, namely, that the hexafluorinated cage **2** is a much more efficient mediator than the parent cage **1** when it comes to electronic interactions between substituents whose ionization potentials are similar to those of the heavier halogens. It would be interesting to probe this experimentally.

Experimental Section

Photoelectron Spectroscopy

PES were recorded on a home-built instrument similar in design to a Perkin–Elmer PS-16. This type of instrument uses an electrostatic cylindrical sector analyzer and a DC capillary discharge in low-pressure He that generates photons with an energy of 21.22 eV (He(I) resonance line). The spectrometer was calibrated periodically during each measurement by injecting a mixture of Ar and Xe into the ionization region. Calibration accuracy is thought to be within ±0.02 eV for IPs listed to two decimal places and ±0.1 eV for those listed to one decimal place. The working resolution was 20–30 meV full width at half maximum for 5-eV electrons (16-eV IP).

General Procedures

Melting points were determined on a Boetius PHMK05 apparatus with a microscope attachment (4 °C min^{-1}). ^{1}H NMR spectra were obtained at 300, 400, and 500 MHz on Varian VXR 300, Bruker 400, and Varian VXR 500 spectrometers, respectively. ^{19}F NMR spectra were obtained at 282.4, 376.5, and 470.7 MHz on Varian VXR 300, Bruker 400, and Varian VXR 500 spectrometers, respectively. ^{13}C NMR spectra were obtained at 100.6 and 125.7 MHz on Bruker 400 and Varian VXR 500 spectrometers, respectively. Samples were dissolved in [D]chloroform unless otherwise indicated. Fluorotrichloromethane, [D]chloroform, and tetramethylsilane were used as internal standards for ^{19}F, ^{13}C, and ^{1}H NMR spectra, respectively, unless otherwise specified. IR spectra were recorded with a Nicolet 800 or Perkin–Elmer FTIR instrument in KBr unless otherwise specified. Electron-impact mass spectra were recorded with an HP 5988A GC–MS instrument. High-resolution and chemical-ionization mass spectra were recorded with a VG 7070EQ instrument. Preparative GC was done in an SE-52 (10% Chromosorb W) 6–20-ft long 0.25″ diameter column.

Reagents

Commercially available tris(trimethylsilyl)silane (Aldrich), *tert*-butyl peroxide (Aldrich), chlorine (Aldrich), aqueous ammonia (Fisher Scientific), and phosphorus pentoxide (Fisher Scientific) were used without purification. The syntheses of **1**,[40] 1,3-Cl_2-**1**,[41] 1,3-Br_2-**1**,[42] 1,3-I_2-**1**,[43] 1,3-$(CN)_2$-**1**,[44] 1,3-Br_2-2,2-Cl_2-**1**,[45] 1,3-Br_2-**2**,[30] and 1,3-I_2-**2**[30] were reported previously.

Syntheses

2: A mixture of 1,3-Br_2-**2**[30] (132 mg, 0.4 mmol), tris(trimethylsilyl)silane (1 mg, 4 mmol), and *tert*-butyl peroxide (1 mg) was sealed in a 5-mL ampoule and heated to 120 °C for 6 h. The ampoule was then secured in an upright position with the bottom quarter immersed in an oil bath for 1 h. The product that sublimed into the upper part of the ampoule was dissolved in a minimal amount of diethyl ether and purified by preparative GC to give 2,2,4,4,5,5-hexafluorobicyclo[1.1.1]pentane (**2**; 53 mg, 76%). M.p.: 38 °C; IR (CS_2): $\tilde{\nu}$ = 928, 2860, 1299, 1244, 1184, 1048, 915, 908 cm^{-1}; ^{1}H NMR: δ = 3.74 ppm (sept, $^3J_{H,F}$ = 1.4 Hz); ^{13}C{^{1}H} NMR: δ = 63.4 (sept, $^2J_{C,F}$ = 19.8 Hz), 109.9 ppm (br t); ^{19}F NMR: δ = −117.2 ppm; MS (EI): *m/z* = 157 (24) $[M-F]^+$, 137 (28), 126 (100), 113 (78), 75 (35), 69 (90); HRMS: *m/z* calcd for $C_5H_2F_6$: 176.0061; found: 176.0073.

1,3-Cl_2-**2**: A solution of **2** (20 mg, 0.11 mmol) in carbon tetrachloride (1 mL) was placed in a 200-mL glass vessel equipped with a gas regulator and a pressure gauge. Air was displaced with argon, and the reaction vessel was filled with chlorine gas to the pressure of 50 psi. The reaction mixture was irradiated with a 150-W tungsten lamp for two weeks. The reaction vessel was cooled in an ice bath, and excess chlorine was carefully released. 1,3-Dichlorohexafluorobicyclo[1.1.1]pentane (1,3-Cl_2-**2**; 6 mg, 22%) was isolated by preparative GC. ^{19}F NMR (CCl_4): δ = −123.2 ppm

(s); $^{13}C\{^{19}F\}$ NMR (CCl_4): $\delta = 53.7$, 109.2 ppm; HRMS: *m/z* calcd for $C_5{}^{35}Cl_2F_6$: 243.9281; found: 243.9304.

1,3-$(CONH_2)_2$-**2**: Aqueous ammonia (30%, 10 mL) was added to a solution of hexafluorobicyclo[1.1.1]pentane-1,3-dicarboxylic acid (1,3-$(COOH)_2$-**2**;[30] 1.46 g, 5 mmol) in THF (10 mL), and the reaction mixture was stirred for 1 h. The solvents were evaporated, and the residue was sublimed at 1×10^{-3} Torr and 80 °C to yield hexafluorobicyclo-[1.1.1]pentane-1,3-carboxamide (1,3-$(CONH_2)_2$-**2**; 1.225 g, 93%). M.p.: 205 °C (decomp.); IR: $\tilde{\nu} = 3390$, 3204, 1681, 1624, 1408, 1226, 113, 958, 918 cm^{-1}; $^{13}C\{^{19}F\}$ NMR ([D$_6$]acetone): $\delta = 71.0$, 111.9, 156.5 ppm; ^{19}F NMR ([D$_6$]acetone): $\delta = -116.4$ ppm; HRMS: *m/z* calcd for $C_7H_2F_6NO_2$: 245.9990 $[M-NH_2]^+$; found: 245.9975.

1,3-$(CN)_2$-**2**: Phosphorus pentoxide (2.8 g, 20 mmol) was thoroughly mixed with 1,3-$(CONH_2)_2$-**2** (262 mg, 1 mmol) in a dry flask. A transfer line terminated with a dry ice-cooled receiver flask was connected to the reaction flask. The mixture was heated to about 200 °C for 0.5 h, and volatile products were accumulated in the receiver flask. The collected product was sublimed in a gradient sublimer at 1 atm and room temperature into the end of the sublimation tube cooled with tap water ($\approx$6 °C) to give 1,3-dicyanohexafluorobicyclo[1.1.1]pentane (1,3-$(CN)_2$-**2**; 86 mg, 38%). M.p.: 58 °C; IR (CS_2) 2256, 1298, 1235, 918, 894, 744 cm^{-1}; ^{13}C NMR: $\delta = 57.87$, 102.37, 110.0 ppm (br t); ^{19}F NMR: $\delta = -111.6$ ppm; MS (CI): $m/z = 226$ $[M]^-$ (18), 207 (100), 188 (42), 169 (21), 157 (23), 141 (11), 127 (99), 113 (52), 99 (28), 73 (27), 58 (26); HRMS: *m/z* calcd for $C_7F_6N_2$: 225.9966; found: 225.9964.

Computational Details

Geometries: The ground-state equilibrium structures of 1,3-Y_2-**1** and 1,3-Y_2-**2** (Y = F, Cl, Br, I, At, CN) were determined by the MP2 method with the Gaussian 94 program.[46] The 6–311G* basis set[47] was used for H, N, C, and F, and the [6s5p] GTOs (Gaussian-type orbitals) of McLean and Chandler[48] were used for Cl. For Br, I, and At atoms, RECP[36,49,50] was used with [2s2p] plus 1d function with $\zeta_d = 0.389$ (Br), 0.266 (I), and 0.225 (At).[51] These optimized structures were used for the calculations of vertical IPs. The equilibrium structures of some ionized states were examined by the UHF/6–31G(d) method.

Photoelectron spectra: The ground and ionized states at these optimized geometries were calculated by the SAC/SAC-CI method. The basis sets of the first-row atoms and H were composed of the [5s3p/3 s] GTOs of Huzinaga[52] and Dunning[53] augmented with 1d polarization functions with $\zeta_d = 0.75$, 0.80, and 0.90 for N, C, and F, respectively. For the other atoms, the same basis sets as in the geometry optimization were used. In the SAC/SAC-CI calculations, the 1s orbitals of C, N, and F and the 1s, 2s, and 2p orbitals of Cl as well as the counterparts of these MOs in the unoccupied manifold were excluded from the active space. To decrease computational effort, configuration selection was performed in the perturbative way.[18] For the ground state, the threshold for the linked terms was $\lambda_g = 1\times10^{-5}$ au, and the unlinked terms were adopted as the products of the important linked terms whose SDCI coefficients were larger than 0.005. For the ionized state, the threshold of the linked term *R* was $\lambda_e = 1\times10^{-6}$ au. The thresholds for the unlinked terms in the SAC-CI were set to 0.1 and 0.001 for selecting the important *R* and *S* operators, respectively. The HF SCF orbitals were obtained with the HONDO8 program,[54] and the SAC-CI calculations were performed with the SAC-CI96 program.[55] The effect of spin–orbit interaction was calculated in the ab initio manner by the method reported previously.[56] Only the one-electron term was included, and only the interaction between singles was evaluated in the SAC-CI wavefunction. Natural-bond-orbital (NBO) analysis of HF/D95 wavefunctions was performed with the NBO routine[38] in the Gaussian 98 program.[57]

Acknowledgements

This study was supported by a Grant for Creative Scientific Research from the Ministry of Education, Culture, Sports, Science, and Technology of Japan and by the US National Science Foundation (CHE-0446688). We are grateful to the JSPS for a grant to the collaborating researchers at Kyoto University, to Mr. Matthew K. MacLeod for performing the NBO calculations, and to Prof. Mark A. Ratner for a useful discussion.

[1] H. M. McConnell, *J. Chem. Phys.* **1961**, *35*, 508–515.
[2] R. Hoffmann, A. Imamura, W. J. Hehre, *J. Am. Chem. Soc.* **1968**, *90*, 1499–1509.
[3] R. Hoffmann, *Acc. Chem. Res.* **1971**, *4*, 1–9.
[4] R. Gleiter, *Angew. Chem.* **1974**, *86*, 770–775; *Angew. Chem. Int. Ed. Engl.* **1974**, *13*, 696–701.
[5] M. N. Paddon-Row, *Acc. Chem. Res.* **1982**, *15*, 245–251.
[6] N. S. Hush, *Coord. Chem. Rev.* **1985**, *64*, 135–157.
[7] R. Gleiter, W. Schäfer, *Acc. Chem. Res.* **1990**, *23*, 369–375.
[8] K. D. Jordan, M. N. Paddon-Row, *Chem. Rev.* **1992**, *92*, 395–410.
[9] V. Coropceanu, N. E. Gruhn, S. Barlow, C. Lambert, J. C. Durivage, T. G. Bill, G. Nöll, S. R. Marder, J.-L. Brédas, *J. Am. Chem. Soc.* **2004**, *126*, 2727–2731.
[10] H. Nakatsuji, K. Hirao, *J. Chem. Phys.* **1978**, *68*, 2053–2065.
[11] a) H. Nakatsuji, *Chem. Phys. Lett.* **1978**, *59*, 362–364; b) H. Nakatsuji, *Chem. Phys. Lett.* **1979**, *67*, 329–333, 334–342.
[12] H. Nakatsuji, *Computational Chemistry: Review of Current Trends*, *Vol. 2*, World Scientific, Singapore, **1997**, pp. 62–124.
[13] H. Nakatsuji, *Acta Chim. Hung.* **1992**, *129*, 719–776.
[14] R. Gleiter, K.-H. Pfeifer, G. Szeimies, U. Bunz, *Angew. Chem.* **1990**, *102*, 418–420; *Angew. Chem. Int. Ed. Engl.* **1990**, *29*, 413–415.
[15] E. Honegger, E. Heilbronner, N. Hess, H.-D. Martin, *Chem. Ber.* **1985**, *118*, 2927.
[16] E. Honegger, E. Heilbronner, N. Hess, H.-D. Martin, *Chem. Ber.* **1987**, *120*, 187.
[17] E. Honegger, E. Heilbronner, T. Urbanek, H.-D. Martin, *Helv. Chim. Acta* **1985**, *68*, 23.
[18] H. Nakatsuji, *Chem. Phys.* **1983**, *75*, 425–441.
[19] H. Nakatsuji, O. Kitao, T. Yonezawa, *J. Chem. Phys.* **1985**, *83*, 723–734.
[20] H. Nakatsuji, M. Ehara, M. H. Palmer, M. F. Guest, *J. Chem. Phys.* **1992**, *97*, 2561–2570.
[21] H. Nakatsuji, M. Ehara, *J. Chem. Phys.* **1994**, *101*, 7658–7671.
[22] M. Ehara, Y. Ohtsuka, H. Nakatsuji, *Chem. Phys.* **1998**, *226*, 113–123.
[23] J. Wan, M. Ehara, M. Hada, H. Nakatsuji, *J. Chem. Phys.* **2000**, *113*, 5245–5252.
[24] M. Ehara, J. Hasegawa, H. Nakatsuji in *Theory and Applications of Computational Chemistry: The First 40 Years* (Eds.: C. E. Dykstra, G. Frenking, K. S. Kim, G. E. Scuseria), Elsevier, Oxford, **2005**, pp. 1099–1141.
[25] M. Levin, P. Kaszynski, J. Michl, *Chem. Rev.* **2000**, *100*, 169–234.
[26] P. F. H. Schwab, M. D. Levin, J. Michl, *Chem. Rev.* **1999**, *99*, 1863–1934.
[27] W. Adcock, A. V. Blokhin, G. M. Elsey, N. H. Head, A. R. Krstic, M. D. Levin, J. Michl, J. Munton, E. Z. Pinkhassik, M. Robert, J.-M. Savéant, A. Shtarev, I. Stibor, *J. Org. Chem.* **1999**, *64*, 2618–2625.
[28] A. J. McKinley, P. N. Ibrahim, V. Balaji, J. Michl, *J. Am. Chem. Soc.* **1992**, *114*, 10631–10637.
[29] a) C. R. Brundle, M. B. Robin, N. A. Kuebler, H. Basch, *J. Am. Chem. Soc.* **1972**, *94*, 1451–1465; b) C. R. Brundle, M. B. Robin, N. A. Kuebler, *J. Am. Chem. Soc.* **1972**, *94*, 1466–1475.
[30] M. D. Levin, S. J. Hamrock, P. Kaszynski, A. B. Shtarev, G. A. Levina, B. C. Noll, M. E. Ashley, R. Newmark, G. G. I. Moore, J. Michl, *J. Am. Chem. Soc.* **1997**, *119*, 12750–12761.
[31] M. D. Levin, P. Kaszynski, J. Michl, *Org. Synth.* **2000**, *77*, 249.
[32] V. V. Bardin, Yu. L. Yagupolskii in *New Fluorinating Agents in Organic Synthesis* (Eds.: L. German, S. Zemskov), Springer-Verlag, Berlin, New York, **1989**, chap. 1.
[33] W. J. Middleton, *J. Org. Chem.* **1975**, *40*, 574–578.
[34] P. Kaszynski, J. Michl, *J. Org. Chem.* **1988**, *53*, 4593–4594.
[35] P. Kaszynski, A. C. Friedli, J. Michl, *J. Am. Chem. Soc.* **1992**, *114*, 601–620.

[36] R. B. Ross, J. M. Powers, T. Atashroo, W. C. Ermler, L. A. LaJohn, P. A. Christiansen, *J. Chem. Phys.* **1990**, *93*, 6654–6670.
[37] K. Kimura, S. Katsumata, Y. Achiba, T. Yamazaki, S. Iwata, *Handbook of HeI Photoelectron Spectra of Fundamental Organic Molecules*, Japan Scientific Societies Press, Tokyo, **1981**.
[38] E. D. Glendening, J. K. Badenhoop, A. E. Reed, J. E. Carpenter, J. A. Bohmann, C. M. Morales, F. Weinhold, NBO Version 5.X, Theoretical Chemistry Institute, University of Wisconsin, Madison, WI (USA), **2003**, to be found under http://www.chem.wisc.edu.
[39] M. A. Bent, *Chem. Rev.* **1961**, *61*, 275–311.
[40] M. R. Rifi, *J. Am. Chem. Soc.* **1967**, *89*, 4442–4445.
[41] K. B. Wiberg, V. Z. Williams, Jr., *J. Org. Chem.* **1970**, *35*, 369–373.
[42] E. W. Della, D. K. Taylor, *J. Org. Chem.* **1994**, *59*, 2986–2996.
[43] F. Alber, G. Szeimes, *Chem. Ber.* **1992**, *125*, 757.
[44] T. Janecki, S. Shi, P. Kaszynski, J. Michl, *Collect. Czech. Chem. Commun.* **1993**, *58*, 89–104.
[45] R. E. Robinson, J. Michl, *J. Org. Chem.* **1989**, *54*, 2051–2053.
[46] M. J. Frisch, G. W. Trucks, H. B. Schlegel, P. M. W. Gill, B. G. Johnson, M. A. Robb, J. R. Cheeseman, T. A. Keith, G. A. Petersson, J. A. Montgomery, Jr., K. Raghavachari, M. A. Al-Laham, V. G. Zakrzewski, J. V. Ortiz, J. B. Foresman, C. Y. Peng, P. Y. Ayala, M. W. Wong, J. L. Andres, E. S. Replogle, R. Gomperts, R. L. Martin, D. J. Fox, J. S. Binkley, D. J. Defrees, J. Baker, J. P. Stewart, M. Head-Gordon, C. Gonzalez, J. A. Pople, Gaussian 94, Gaussian Inc., Pittsburgh, PA (USA), **1994**.
[47] R. Krishnan, J. S. Binkley, R. Seeger, J. A. Pople, *J. Chem. Phys.* **1980**, *72*, 650–654.
[48] A. D. McLean, G. S. Chandler, *J. Chem. Phys.* **1980**, *72*, 5639–5648.
[49] M. M. Hurley, L. F. Pacois, P. A. Christiansen, R. B. Ross, W. C. Ermler, *J. Chem. Phys.* **1986**, *84*, 6840–6953.
[50] L. A. LaJohn, P. A. Christiansen, R. B. Ross, T. Atashroo, W. C. Ermler, *J. Chem. Phys.* **1987**, *87*, 2812–2824.
[51] S. Huzinaga, J. Andzelm, M. Klobukowski, E. Radzio-Andzelm, Y. Sakai, H. Tatewaki, *Gaussian Basis Sets for Molecular Calculations*, Elsevier, Amsterdam, **1984**.
[52] S. Huzinaga, *J. Chem. Phys.* **1965**, *42*, 1293–1302.
[53] T. H. Dunning, Jr., *J. Chem. Phys.* **1970**, *53*, 2823–2833.
[54] M. Dupuis, A. Farazdel, HONDO8 program system, A. MOTECC-91, Center for Scientific and Engineering Computations, IBM Corporation, Kingston, NY (USA), **1991**.
[55] H. Nakatsuji, M. Hada, M. Ehara, J. Hasegawa, T. Nakajima, H. Nakai, O. Kitao, K. Toyota, SAC/SAC-CI program system (SAC-CI96) for calculating ground, excited, ionized, and electron-attached states with singlet-to-septet spin multiplicities, Kyoto University, Kyoto (Japan), **1996**.
[56] H. Nakatsuji, Y. Matsuzaki, T. Yonezawa, *J. Chem. Phys.* **1988**, *88*, 5759–5769.
[57] M. J. Frisch, G. W. Trucks, H. B. Schlegel, G. E. Scuseria, M. A. Robb, J. R. Cheeseman, V. G. Zakrzewski, J. A. Montgomery, Jr., R. E. Stratmann, J. C. Burant, S. Dapprich, J. M. Millam, A. D. Daniels, K. N. Kudin, M. C. Strain, O. Farkas, J. Tomasi, V. Barone, M. Cossi, R. Cammi, B. Mennucci, C. Pomelli, C. Adamo, S. Clifford, J. Ochterski, G. A. Petersson, P. Y. Ayala, Q. Cui, K. Morokuma, D. K. Malick, A. D. Rabuck, K. Raghavachari, J. B. Foresman, J. Cioslowski, J. V. Ortiz, B. B. Stefanov, G. Liu, A. Liashenko, P. Piskorz, I. Komaromi, R. Gomperts, R. L. Martin, D. J. Fox, T. Keith, M. A. Al-Laham, C. Y. Peng, A. Nanayakkara, C. Gonzalez, M. Challacombe, P. M. W. Gill, B. Johnson, W. Chen, M. W. Wong, J. L. Andres, C. Gonzalez, M. Head-Gordon, E. S. Replogle, J. A. Pople, Gaussian 98, Revision A.11.4, Gaussian Inc., Pittsburgh, PA (USA), **2002**.

Received: December 12, 2006
Published online: June 28, 2007

